Uptake of Dextran-Coated Monocrystalline Iron Oxides in Tumor Cells and Macrophages

Anna Moore, PhD • Ralph Weissleder, MD, PhD • Alexei Bogdanov, Jr., PhD

Although several dextran-coated iron oxide preparations are in preclinical and clinical use, little is known about the mechanism of uptake into cells. As these particles have been shown to accumulate in macrophages and tumor cells, we performed cellular uptake and inhibition studies with a prototypical monocrystalline iron oxide nanoparticle (MION). MION particles were labeled with fluorescein isothiocyanate or radioiodinated and purified by gel permeation chromatography. Two preparations of MION particles were used in cell experiments: nontreated MION and plasma-opsonized MION purified by gradient density purification. As determined by immunoblotting, opsonization resulted in C3, vitronectin, and fibronectin association with MION. Incubation of cells with fluorescent MION showed active uptake of particles in macrophages both before and after opsonization. In C6 tumor cells, however, intracellular MION was only detectable in dividing cells. Quantitatively, ^{125}I-labeled MION was internalized into cells with uptake values ranging from 17 ng (in 9L gliosarcoma) to 970 ng iron per million cells for peritoneal macrophages. Opsonization increased MION uptake into macrophages sixfold, whereas it increased the uptake in C6 tumor cells only twofold. Results from uptake inhibition assay suggest that cellular uptake of nonopsonized (dextran-coated) MION particles is mediated by fluid-phase endocytosis, whereas receptor-mediated endocytosis is presumably responsible for the uptake of opsonized (protein-coated) particles.

Index terms: Iron oxide • Dextran • Opsonization • Endocytosis

JMRI 1997; 7:1140–1145

Abbreviations: BBB = blood-brain barrier, BSA = bovine serum albumin, DMEM = Dulbecco's modified Eagle's medium, DMSO = dimethyl sulfoxide, DTT = dithiothreitol, EDTA = ethylenediaminetetraacetic acid, FBS = fetal bovine serum, FITC = fluorescein isothiocyanate, HBSS = Hanks' balanced salt solution, HPLC = high-performance liquid chromatography, MION = monocrystalline iron oxide nanoparticle, NEM = *N*-ethylmaleimide, PBS = phosphate-buffere solution, PVDF = polyvinylidene difluoride, RES = reticuloendothelial system, RPMI = Roswell Park Memorial Institute, SDS-PAGE = sodium dodecyl sulfate polyacrylamide gel electrophoresis, Tris = tris(hydroxymethyl)aminomethane.

From the Center for Molecular Imaging Research (CMIR), Department of Radiology, Massachusetts General Hospital, 149 13th Street, Room 5403, Charlestown, MA 02129. Received March 11, 1997; revision requested July 9; revision received July 17; accept July 18. Supported by National Institutes of Health Grants RO1-CA-59649-04 and RO1-CA-54886-05. **Address reprint requests to** R.W.

DEXTRAN-COATED MONOCRYSTALLINE iron oxide nanoparticles (MION) (1) and dextran-grafted copolymers (2) are currently being used as magnetic labels for MRI of neoplasia (reviewed in ref. 3). The dextran coating of these drug carriers was chosen because of its biocompatibility, prior experience with dextrans in human use, and the relative stability of dextran-coated particles and graft copolymers. In vivo, dextran-coated magnetic particles have been shown to accumulate primarily in phagocytic cells in liver, spleen, bone marrow, and lymph nodes after intravenous administration (4). We have also observed that the uptake of dextran-covered particles is not limited to "professional" phagocytes in these organs but also occurs in many other cells in culture and in vivo, depending on the mode of delivery (5). For example, MION particles are avidly taken up by neurons and astrocytes after blood-brain barrier (BBB) disruption or direct injection into the brain (6). Moreover, upon the loss of blood-brain barrier integrity, MION particles are capable of accumulation in CNS tumor cells (7,8). Previously, we have demonstrated that once internalized, MION is initially located in the tubular lysosomal compartment as evidenced by co-localization of fluorescent-labeled MION and anti-lysosomal specific glycoprotein antibodies (9). The goal of the present study was to perform a comparative analysis of MION uptake in different cell lines. Specifically, we were interested in elucidating the mechanism and quantitating MION uptake in tumor cells and macrophages, the latter representing an accessory cell population that is often recruited by tumors (10,11). For this purpose, we labeled MION radioactively and/or fluorescently and performed cell uptake and inhibition studies and fluorescence microscopy, respectively.

• MATERIALS AND METHODS

Cell Lines and Primary Cell Cultures

Two different categories of cells were used: nonproliferating primary cultures (macrophages) and proliferating tumor cell lines (C6, 9L, LX-1, J-774). Peritoneal macrophages were obtained from BALB/c mice (Charles River Labs, Wilmington, MA) by peritoneal lavage with a sterile sucrose solution (.34 M). Cells were resuspended in Dulbecco's modified Eagle's medium (DMEM; Cellgro, Mediatech, Washington, DC), with 10% fetal bovine serum (FBS; Cellgro), and cultured for 3 to 4 days.

Rat C6 glioma cells (CCL 107, ATCC) and 9L gliosarcoma cells (Brain Tumor Research Center, San Francisco, CA) (12) were also grown in DMEM with 10% FBS. LX-1 human small cell lung carcinoma cells (13) were grown in Roswell Park Memorial Institute (RPMI) 1640 medium (Cellgro) supplemented with 10% FBS.

MION Synthesis and Labeling

MION-46 was synthesized as described in ref. 1. Briefly, to a solution containing dextran T-10 (produced by Leuconostoc mesenteroides strain B512, 500 mg/ml, Pharmacia, Uppsala, Sweden), ferric chloride hexahydrate (33 mg/ml), and ferrous chloride tetrahydrate (12 mg/ml) (Sigma, St. Louis, MO), a 30% solution of ammonium hydroxide was added to shift the pH to 12. The resultant colloid was then washed using 30-kD hollow fiber filtration cartridges (H1P30-43, Amicon, Beverly, MA) until the iron oxide colloid was free of dextran. From this stock solution, monocrystalline nanoparticles were recovered by ultrafiltration using hollow membrane cartridges (H1MP01-43, Amicon, Beverly, MA). The characteristics of the resultant colloid and the physicochemical properties of MION have been described in more detail elsewhere (1).

MION was labeled with ^{125}I to quantify iron uptake by the cells. Iodination of MION and opsonized MION was performed with $Na^{125}I$ (574 mCi/mM of iron, .1 M sodium carbonate, pH 9.0) in the presence of IodoGen (Pierce, Rockford, IL). Both compounds were purified after iodination by gel filtration through Sephadex G-25m column saturated with bovine serum albumin (BSA).

Labeling with fluorescein isothiocyanate (FITC; Molecular Probes, Eugene, OR) was achieved by adding 30 mg FITC in .5 ml dimethyl sulfoxide (DMSO) to 5 ml of MION solution (6 mg Fe/ml, .1 M sodium carbonate, pH 11) with subsequent purification using ultrafiltration (YM-100, Amicon, Beverly, MA) and gel filtration on Sephadex G-25m immediately before use.

MION Opsonization

Fresh rat or mouse plasma (1 ml) was incubated with ^{125}I-MION (2 mg Fe in Hanks' balanced salt solution [HBSS]) for 30 minutes at 37°C and then cooled on ice. Opsonized MION was purified by sedimentation through a 7.5% to 18% gradient of sodium metrizoate in Ca and Mg containing HBSS for 16 hours at 35,000 g, 4°C, using a SW41Ti rotor (Beckman, Columbia, MD). The precipitate was washed with HBSS by centrifugation for 1 hour under the same conditions. After centrifugation the iron-rich band was redissolved in HBSS and analyzed by high-performance liquid chromatography (HPLC) on a SEC-5 size-exclusion column (Rainin Inst. Co., Medford, MA). Iron and protein determinations were performed as described previously (14). Radioiodinated MION was passed through Sephadex G-25m spin column immediately before addition to cells. The specific activity of samples was determined by gamma-counting (1282 Compugamma CS, LKB Wallac, Sweden).

Immunoblotting

Thirty μg of total MION-associated protein was dissolved in 5% SDS, 25 mM of dithiothreitol (DTT), 5 mM of ethylenediaminetetraacetic acid (EDTA) in .1 M of tris(hydroxymethyl)aminomethane (Tris), pH 7 by boiling, subjected to sodium dodecyl sulfate-polyacrylamide gel electrophoresis (SDS-PAGE) on 10% gels and transferred onto polyvinylidene difluoride (PVDF) membranes (Bio-Rad Labs, Hercules, CA) by electroblotting. Membranes were blocked with 5% blocker (defatted milk, Bio-Rad) in .1% Tween phosphate buffered solution (PBS). Blots were incubated for 1 hour in the presence of diluted primary antisera against rat or mouse plasma proteins (Chemicon, Tamecula, CA, or Cappel, Durham, NC, at 1:200 dilution in 1% blocker) followed by biotinylated secondary antibodies (dilution: 1:1,000, Pierce) and avidin-peroxidase (dilution: 1:1000, Bio-Rad). Bands were visualized using a chloronaphthol/diaminobenzidine mixture (15).

Cell Uptake Assay

Cells (10^6 cells/well) were incubated with freshly prepared nonopsonized or opsonized ^{125}I-MION at various concentrations in serum-free DMEM. Cell suspensions were incubated at 37°C for 1 hour and then washed three times by centrifuging through a step gradient of 40% Histopaque-1077 (Sigma) in HBSS. After the final centrifugation and aspiration of the supernatant, radioactivity associated with cell pellets was determined and normalized for protein content. Anchorage-dependent cells (C6 glioma, 9L gliosarcoma, J-774) were grown in 24 well plates (Falcon, Becton Dickinson, Lincoln Park, NJ). MION was added in .5 ml of serum-free DMEM, incubated as described above, and washed with HBSS three times, and cells were lysed in .5 ml of 1% Triton X-100, 1 mM of EDTA, pH 8 before radioactivity/protein determinations.

Uptake Inhibition Assays

C6 glioma cells and peritoneal mouse macrophages (10^6 cells/well) were plated onto 24 well plates in .5 ml of DMEM with 10% FBS. Immediately before the MION addition, cells were washed with HBSS to remove serum proteins. Unlabeled MION (200 μg Fe/well), rat plasma (30 μg/well of plasma proteins), and dextran T10 (200 μg/well) served as inhibitors and were added to the cells immediately before the addition of ^{125}I-MION and opsonized ^{125}I-MION (20 μg Fe/well). In another experiment, *N*-ethylmaleimide (NEM) (16) was added to the cells for 10 minutes, before addition of ^{125}I-MION or opsonized ^{125}I-MION. After the incubation (1 hour, 37°C), supernatants were aspirated, and cells were washed in HBSS three times, collected, and counted in a gamma counter.

Fluorescence Microscopy

C6 glioma cells and peritoneal macrophages were plated on glass coverslips at 30% to 35% confluency. Cells were incubated for 1 hour in DMEM without phenol red containing fluorescent labeled MION (18 mM Fe) at 37°C. After incubation, coverslips were washed extensively with HBSS and mounted in a thermostated chamber. Fluorescence images were obtained as described previously (9).

• RESULTS

Opsonization of MION

In an initial experiment, we determined the amount and type of protein binding to dextran-coated iron oxide particles. Opsonized MION preparations contained .14 ± .05 μg bound plasma proteins per μg of iron as determined by the protein assay. Size-exclusion HPLC analysis of opsonized and nonopsonized MION preparations is shown in Figure 1. The first eluted peak accounts for MION separated from traces of free dextran and glucose (second and third peaks, respectively). MION and opsonized-MION peaks were shifted with respect to each other corresponding to a 25% increase in median effective hy-

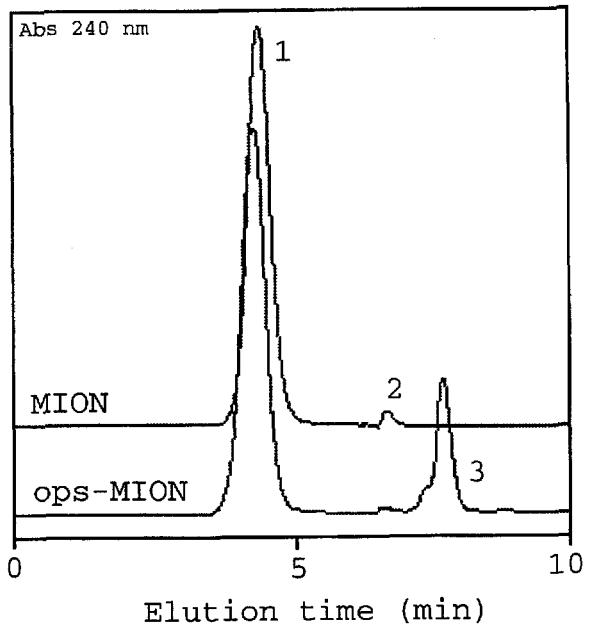

Figure 1. Size-exclusion HPLC (SEC-5, Rainin Inst. Co, Medford, MA) of MION (.1 mg Fe/ml, upper trace) and opsonized MION (.1 mg Fe/ml, lower trace). 1 = MION, 2 = dextran, 3 = glucose. Eluent: 1 mg/ml, .05 M sodium phosphate, pH 6.0.

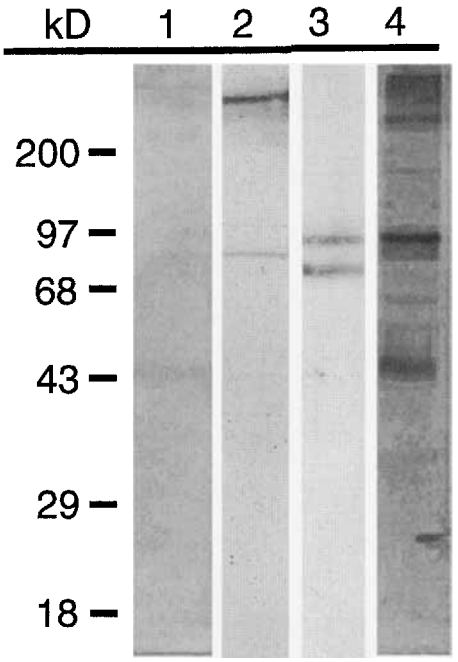

Figure 2. Immunoblotting of opsonized MION samples with polyclonal antisera against 1: transferrin (1), vitronectin (2), fibronectin (3), complement C3 (4). Thirty μg total MION-associated protein/lane were resolved 10% polyacrylamide gel and transferred onto PVDF membranes (Bio-Rad Labs, Hercules, CA). Membranes were probed with primary antisera, biotinylated secondary antibodies, and avidin peroxidase.

drodynamic diameter (Fig. 1). This shift accounts for an increase of median particle weight from .75 to 1.01 MDa, according to a calibration of the column with globular proteins. Immunoblotting of opsonized MION samples revealed the bound proteins to be fibronectin, vitronectin, and C3 (with heavy chain, light chain, and C3dg fragments present). The extent of vitronectin binding detectable by immunoblotting was time dependent and increased during storage at 4°C (1–3 weeks). There was no detectable transferrin binding characteristic for iron oxide preparations with short blood half-life in vivo (17), (Fig. 2, lane 1).

Quantitation of Cellular MION Uptake

To compare cellular uptake in different cell lines, MION was used at a concentration of 1 mg Fe/10^6 cells. This concentration of iron was nontoxic for all cells, as determined in prior viability assays. As expected, uptake was highest for the primary peritoneal macrophages and J-774 cells known to have high phagocytic activity (18). Importantly, tumor cells also showed MION uptake, but to a lesser degree than other cells tested. Overall uptake ranged from 5×10^4 particles/cell to approximately 5×10^6 particles/cell (Table 1).

Effect of Opsonization on Cellular Uptake

The effect of opsonization on MION cell uptake was subsequently compared for the primary peritoneal macrophage culture and C6 tumor cell line. Over a concentration range of .05 to 25 μg Fe/10^6 cells, we observed a very similar concentration-dependent uptake for nonopsonized MION in C6 glioma and macrophages (Fig. 3). Opsonization of MION increased macrophage uptake sixfold (from 49 ± 2 ng to 301 ± 38 ng Fe/10^6 cells), whereas it increased uptake into C6 cells only twofold (from 27 ± 2 ng to 58 ± 5 ng Fe/10^6 cells).

Competition Assays

To differentiate between several potential cell uptake pathways, we used inhibitors or inhibitive conditions known to affect one or the other pathway (Figs. 4A and 4B): NEM (inhibitor of vesicular traffic), dextran (coat component of MION), plasma proteins (opsonization components), and nonopsonized unlabeled MION. We limited this study to opsonized iron oxide because MION rapidly binds to plasma proteins after intravenous administration. In macrophages (Fig. 4A), NEM caused a dramatic decrease in uptake (72%, ie, 86 ng Fe/10^6 cells versus 301 ng Fe/10^6 cells; $P < .05$). Plasma protein inhibition resulted in a smaller reduction of cell uptake (32%, ie, 210 ng Fe/10^6 cells versus 301 ng Fe/10^6 cells; $P < .5$). Incubations performed in the presence of dextran or nonopsonized MION did not result in any detectable uptake inhibition. In C6 cells (Fig. 4B), both NEM and plasma-reduced cell uptake (30% of 39 ng Fe/10^6 cells versus 58 ng Fe/10^6 cells; $P < .5$). The other compounds studied did not result in any significant reduction of opsonized MION uptake in C6 cells.

Fluorescence Microscopy

Using a covalent conjugate of MION and FITC, we studied the morphology of intracellular MION before and after the opsonization (Figs. 5 and 6). In C6 cells, the nonopsonized MION was localized predominantly in large pinosomes and only in a subpopulation of postmitotic cells (Figs. 5A and 5B). Opsonized MION was primarily localized to perinuclear vesicles, some of them large, resembling macropinosomes (Figs. 5C and 5D). In macrophages, the uptake was more homogenous (Figs. 6A and 6B). In many macrophages, fluorescent tubular lysosomes were detectable (Fig. 6A, inset) identical to previously described structures, when macrophages were incubated with ovalbumin-MION (9). The fluorescent images of macrophages showed very extensive accumulation of MION in peripheral macropinosomes as well as in perinuclear phagolysosomes (Figs. 6C and 6D).

Table 1
Cellular Uptake of Nonopsonized MION Particles by Different Malignant and Primary Cell Lines

Cell Line or Primary Cell Culture	Species	MION Uptake (ng Fe/10^6 cells)[a]	MION (particles/cell)[b]
9L Gliosarcoma	rat	17	85,000
C6 Glioma	rat	25	125,000
LX-1 Small cell lung carcinoma	human	58	290,000
J-774 Macrophage-like cells	mouse	310	1,550,000
Peritoneal macrophages	mouse	970	4,850,000

[a]1 mg Fe/10^6 cells added in serum-free DMEM and incubated for 1 hour at 37°C.
[b]Estimated assuming a mean particle core size of 4.6 nm (1).

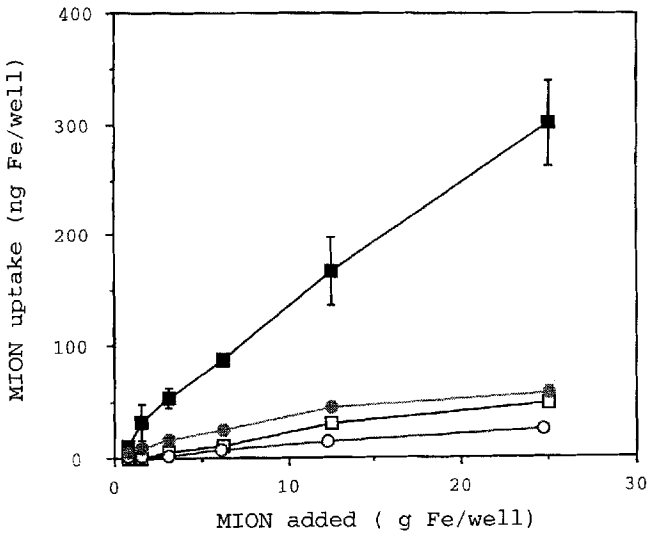

Figure 3. Comparative uptake of MION (open symbols) and opsonized MION (solid symbols) by macrophages (squares) and C6 glioma cells (circles) (10^6 cells/well).

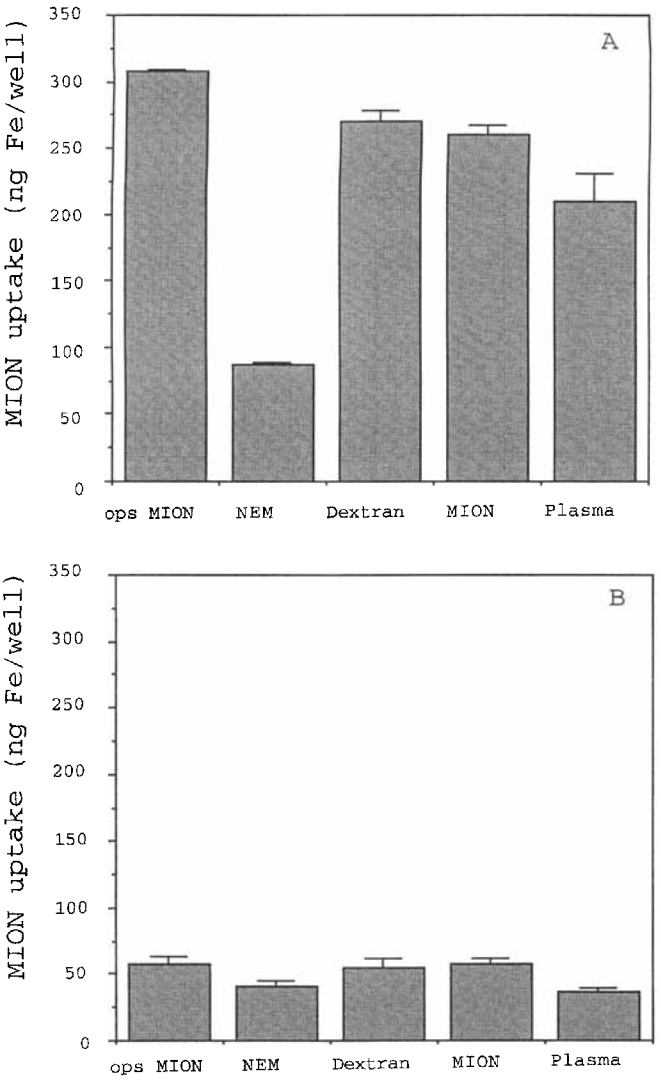

Figure 4. Competitive inhibition of opsonized MION uptake in macrophages (**A**) and in C6 cells (**B**). Cells were plated in 24 well plates and incubated with opsonized MION in the presence of corresponding inhibitors for 1 hour at 37°C.

• DISCUSSION

We have previously demonstrated that MION particles extravasate into the interstitium of some solid tumors, eg, experimental rodent gliomas (7), and that these particles accumulate within tumor cells located adjacent to vessels. Because the endocytosis rate in tissues depends on cell viability and proliferation (eg, the uptake in actively growing tumor regions is far more likely than in necrotic regions), it has been suggested that tumor cell uptake ("tumor cell endocytosis") may serve as an important prognostic factor in cancer diagnosis and the evaluation of cancer therapy (19). In the present study, we quantitated MION uptake of particle/plasma binding on cell uptake.

Plasma Protein Binding

The efficiency of cell uptake of particles in culture depends primarily on particle size as well as the surface characteristics, which in turn, determine opsonization patterns (20). In previous studies, it had been demonstrated that the dextran coat from leuconostoc mesenteroides of iron oxide particles is not inert and binds several plasma proteins (14,17). The current, more detailed immunoblotting experiments revealed that the absorbed (opsonized) protein fraction consists of C3 component, vitronectin, and fibronectin. Cell uptake studies confirmed that this opsonization significantly contributes to the cellular uptake in macrophages, being sixfold higher for opsonized versus nonopsonized particles.

Tumor Cells

Phagocytic activity in tumor cells was first investigated in glial cells in vitro (5). This activity of tumor cells has been used to explain the progressive disappearance of host tissue during invasion and is believed to account for the small amount of necrosis in host tissues replaced by invading malignant cells (21). In the present study, we have shown that C6 glioma cells can actively internalize nonopsonized dextran-coated iron oxide particles. As shown by fluorescence microscopy, the uptake is detectable in proliferating cells (22) and may be explained by fluid phase endocytosis in the G1 cell cycle phase (22,23). The uptake of MION by glioma cells was slightly increased by opsonization, a finding that was initially unsuspected. This observation may be explained by (*a*) the contribution of receptor-mediated uptake or (*b*) the overall enhancement of fluid phase endocytosis of MION particles as a result of the larger size of opsonized particles (24,25). Results from the performed inhibition experiments are further evidence that MION is indeed internalized by C6 tumor cells (inhibition of intracellular

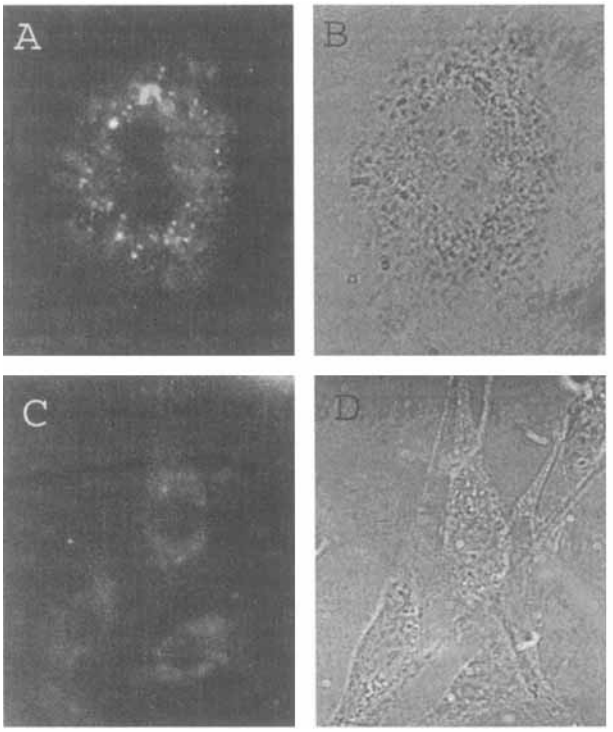

Figure 5. Fluorescent microscopy images of FITC-labeled MION uptake by C6 cells. MION (1 mg/ml) was incubated with cells for 1 hour in complete medium and cells were washed in HBSS. **(A, B)** Native preparation; **(C, D)** MION opsonized with rat plasma.

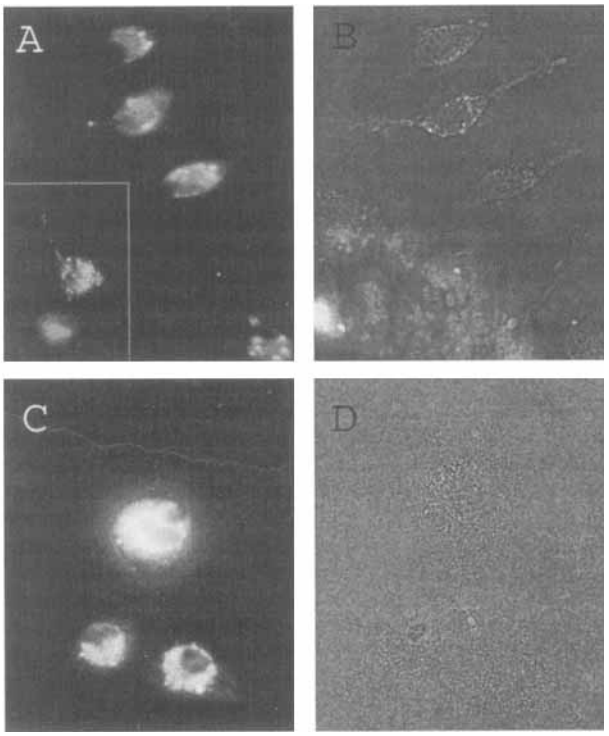

Figure 6. Fluorescent microscopy images of FITC-labeled MION uptake by peritoneal macrophages. MION (1 mg/ml) was incubated with cells for 1 hour in complete medium and cells were washed in HBSS. **(A, B)** Native preparation; **(C, D)** MION opsonized with mouse plasma. Inset **(A)**: accumulation in tubular lysosomes.

vesicular transport by NEM) (16,26), and that the uptake is at least partially mediated by opsonized MION binding to the cell surface (plasma inhibition).

Macrophages

Because scavenger (27) and complement receptors (28) are prominent on macrophage plasma membranes, it is likely that opsonized MION is recognized by these receptors and is actively taken up by receptor-mediated endocytosis. In the present study, we have shown that NEM significantly reduces (72% decrease) cellular internalization of opsonized MION. Fluorescence microscopy confirmed that opsonized MION (Fig. 6B) is localized within macropinosomes or phagosomes. Inhibition experiments demonstrated that plasma proteins compete with opsonized MION uptake presumably by binding to macrophage receptors. In turn, the competition experiment with dextran and nonopsonized unlabeled MION did not reveal any significant inhibition of endocytosis. These findings support the observation that there are no known binding centers for either free dextran or for dextran coated iron oxide particles on the macrophage plasma membrane.

Macrophages in Tumors

Many solid tumors contain macrophages, an accessory cell population that is actively recruited in tumors in vivo (10). Tumoral uptake of dextran-coated iron oxide particles in vivo may thus occur both in tumor cells as well as in tumor-associated macrophages. Recent studies have shown that the degree of intratumoral infiltration and distribution of phagocytic cells is a function of different factors, such as the level of MCP-1 (monocyte chemoattractant protein-1) expression (29), cytokine production in situ (30), or the stage of the tumor development and angiogenesis (10). The population of active phagocytes (macrophages) in tumors has been estimated to be approximately .5% of the total cancer cells, whereas approximately 15% to 20% of cancer cells are proliferating at any given time (31). Assuming that macrophage uptake of particles is roughly 20 times more effective than tumor cell uptake, the small macrophage resident population may add up to up to half of cell internalized particles in a solid tumor, primarily due to the very efficient scavenging of opsonized particles. However, if the interaction of the diagnostic agent with plasma components is minimized (32), the impact of phagocytic cell subpopulations on accuracy of "tumor cell endocytosis imaging" will be considerably lower.

Implications for Imaging

There are several implications of the current research on MRI using dextran-coated iron oxides as contrast agents. First, the widely believed notion that iron oxides only accumulate in cells of the reticuloendothelial system is not true. In fact, accumulation in non-reticuloendothelial system (RES) cells can be prominent enough to allow for cell labeling in vitro (11) or even in vivo (7,19). For example, dextran-coated iron oxides accumulate in brain tumor cells after iv administration, an observation that can be used to improve the delineation of the true tumor border (19). In addition, tumors in non-RES-containing organs (eg, colon tumors, pelvic tumors, etc.) accumulate such iron oxides, which may improve local staging accuracy. Second, the relaxivity of iron oxide agents (and thus their MRI features) varies considerably, depending on whether a given agent is internalized inside a cell or exists in solution, eg, in interstitial fluid (11).

Whereas R1 effects predominate in solution, particles internalized into a tumor cells predominantly exert R2* effects. Because the fluid-phase endocytosis is more prominent in proliferating cells (dependent on the cell cycle phase) (34), MRI may potentially be used to establish tumor growth kinetics by estimating intracellular/extracellular fractions of iron oxides. Finally, the biodistribution and blood half-lives of different iron oxide preparations may be, in large part, governed by the different degrees of opsonization. Prior research (14), as well as this study, confirms that the density of the dextran coat influences blood half-life, with a denser coat increasing it (17). This observation bears implications on the future development of long circulating iron oxide preparations, ie, those particularly useful for MR angiography, functional imaging, or imaging of tumor cell endocytosis.

References

1. Shen T, Weissleder R, Papsiov M, Bogdanov A, Brady T. Monocrystalline iron oxide nanocompounds (MION): physiochemical properties. Magn Reson Med 1993; 29:599–604.
2. Harika L, Weissleder R, Poss K, Papisov M. Macromolecular intravenous contrast agent for MR lymphography: characterization and efficacy studies. Radiology 1996; 198:365–370.
3. Weissleder R, Bogdanov A, Papisov M. Drug targeting in magnetic resonance imaging. In: Torchilin V, ed. Handbook of targeted delivery of imaging agents. Boca Raton, FL: CRC Press Inc., 1995; 133–147.
4. Weissleder R, Bogdanov A, Papisov M. Drug targeting in MR imaging. Magn Reson Q 1992; 8:55–63.
5. Noske W, Lentzen H, Lange K, Keller K. Phagocytic activity of glial cells in culture. Exp Cell Res 1982; 142:437–445.
6. Neuwelt E, Weissleder R, Nilaver G, et al. Delivery of virus-sized iron oxide particles to rodent CNS neurons. Neurosurgery 1994; 34:777–784.
7. Zimmer C, Weissleder R, Poss K, Bogdanova A, Wright SC, Enochs WS. MR imaging of phagocytosis in experimental glioma. Radiology 1995; 197:533–538.
8. Neuwelt E, Barnett P, Hellström K, Hellström I, McCormick C, Ramsey F. Effect of blood-brain barrier disruption on intact and fragmented monoclonal antibody localization in intracerebral lung carcinoma xenografts. J Nucl Med 1994; 35:1831–1841.
9. Schulze E, Ferrucci J, Poss K, LaPointe L, Bogdanova A, Weissleder R. Cellular uptake and trafficking of a prototypical magnetic iron oxide label in vitro. Invest Radiol 1995; 30:604–610.
10. Blood CH, Zetter BR. Tumor interactions with the vasculature: angiogenesis and tumor metastasis. Biochim Biophys Acta 1990; 1032:89–118.
11. Weissleder R, Cheng H, Bogdanova A, Bogdanov A Jr. Magnetically labeled cells can be detected by MR imaging. J Magn Reson 1997; 7:258–263.
12. Wheeler K, Tel N, Williams M, Sheppard S, Levin V, Kabra P. Factors influencing the survival of rat brain tumor cells after in vitro treatment with 1,3-bis(2-chloroethyl)-1-nitrosourea. Cancer Res 1975; 35:1464–1469.
13. Ovejera A, Houchens D. Human tumor xenografts in athymic nude mice as a preclinical screen for anticancer agents. Semin Oncol 1981; 8:386–393.
14. Bogdanova A, Nossiff N, Bogdanov A, Brady T, Weissleder R. The role of opsonins in cellular uptake of dextran stabilized superparamagnetic iron oxides. In: Proceedings of the 2nd annual meeting of the Society of Magnetic Resonance in Medicine. San Francisco: Society of Magnetic Resonance in Medicine 1994; 931.
15. Young P. An improved method for the detection of peroxidase-conjugated antibodies on immunoblots. J Virol Methods 1989; 24:227–235.
16. Goda Y, Pfeffer S. Identification of a novel N-ethylaleimide-sensitive cytosolic factor required for vesicular transport from endosomes to the trans-Golgi network in vitro. J Cell Biol 1991; 112:823–831.
17. Bogdanov A, Papisov M, Weissleder R, Shen T, Brady T. Opsonization of dextran stabilized iron oxides with plasma proteins. In: Proceedings of the 11th annual scientific meeting of the Society of Magnetic Resonance in Medicine. Berlin: Society of Magnetic Resonance in Medicine, 1992; 864.
18. Schwarzbaum S, Diamond, B. The J774.2 cell line presents antigen in a I region restricted manner. J Immunol 1983; 131: 674–677.
19. Zimmer C, Wright S, Engelhardt R, et al. Tumor cell endocytosis imaging facilitates delineation of glioma-brain interface. Exp Neurol 1997; 143:61–69.
20. Rabinovich M. Professional and non-professional phagocytes: an introduction. Trends Cell Biol 1995; 5:85–87.
21. Bjerknes R, Bjerkvig R, Laerum O. Phagocytic capacity of normal and malignant rat glial cells in culture. J Natl Cancer Inst 1987; 78:279–294.
22. Berlin R, Oliver J, Walter R. Surface functions during mitosis I: phagocytosis, pinocytosis and mobility of surface-bound Con A. Cell 1978; 15:327–341.
23. Quintart J, Leroy-Houyet MA, Trouet A, Baudhuin P. Endocytosis and chloroquine accumulation during the cell cycle of hepatoma cells in culture. J Cell Biol 1979; 82:644–653.
24. Pratten M, Lloyd J. Pinocytosis and phagocytosis: the effect of size of a particulate substrate on its mode of capture by rat peritoneal macrophages cultured in vitro. Biochim Biophys Acta 1986; 881:307–313.
25. Berthiaume EP, Medina C, Swanson JA. Molecular size-fractionation during endocytosis in macrophages. J Cell Biol 1995; 129:989–998.
26. Diaz R, Mayorga LS, Weidman PJ, Rothman JE, Stahl PD. Vesicle fusion following receptor-mediated endocytosis requires a protein active in Golgi transport. Nature 1989; 339: 398–400.
27. Kodama T, Freeman M, Rohrer L, Zabrecky J, Matsudaira P, Krieger M. Type I macrophage scavenger receptor contains α-helical and collagen-like coiled coils. Nature 1990; 343:531–535.
28. Shevach E. Macrophages and other accessory cells. In: Paul WE, ed. Fundamental immunology. New York: Raven Press, 1984; 72–75.
29. Takeshima H, Kuratsu J, Takeya M, Yoshimura T, Ushio Y. Expression and localization of messenger RNA and protein for monocyte chemoattractant protein-1 in human malignant glioma. J Neurosurg 1994; 80:1056–1062.
30. Camp BJ, Dyhrman ST, Memoli VA, Mott LA, Barth RJ Jr. In situ cytokine production by breast cancer tumor-infiltrating lymphocytes. Ann Surg Oncol 1996; 3:176–184.
31. Brown RS, Leung JY, Fisher SJ, Frey KA, Ethier SP, Wahl RL. Intratumoral distribution of tritiated fluorodeoxyglucose in breast carcinoma: I. Are inflammatory cells important? J Nucl Med 1995; 36:1854–1861.
32. Weissleder R, Bogdanov A, Papisov M. Long-circulating iron oxides for MR imaging. Adv Drug Delivery Rev 1995; 16:321–334.